

Robust design of an optical router based on a tapered side-coupled integrated spaced sequence of optical resonators

P. Bettotti,* M. Mancinelli, R. Guider, M. Masi, M. Rao Vanacharla, and L. Pavesi

Nanoscience Laboratory, Department of Physics, University of Trento, via Sommarive 14, 38123 Povo, Trento, Italy

*Corresponding author: bettotti@science.unitn.it

Received January 4, 2011; revised March 1, 2011; accepted March 16, 2011;
 posted March 17, 2011 (Doc. ID 140536); published April 15, 2011

A novel (to our knowledge) scheme of an optical router/switch element, composed of a tapered side-coupled integrated spaced sequence of optical resonators, is proposed. It is based on a modified design of the ring sequence in which the resonance conditions are set by the single ring resonance and by the coherent feedback of the sequence of rings. This double condition yields robustness against fabrication defects, dense routing capability, and high switching efficiency. © 2011 Optical Society of America
 OCIS codes: 130.3120, 220.4241, 250.6715.

Integrated photonics can overcome one of the most important limitations of electronics. In fact, the multicore paradigm has changed the performance metric from the CPU clock frequency to the rate of data exchange [1]. The integration of photonics with electronics allows us to increase the available bandwidth and reduce both power consumption and latency [2,3]. Among the building blocks of photonic integrated circuits, routers and switches are the foundations of data management. Considering the future target of 100 terabytes/s [4], routers and switches will assume an even more important role. In this Letter, we present an innovative and robust design of a router/switch device suitable for on-chip dense wavelength division multiplexing with 50 GHz channel spacing. The design exploits the coupled-resonator-induced transparency (CRIT) that occurs in a tapered side-coupled integrated spaced sequence of optical resonators (SCISSOR) structure. In this tapered SCISSOR (TS), each ring has a slightly different radius from its neighbors [5]. Moreover, only a single pair of rings is spaced by a length that allows constructive interference to yield a CRIT resonance (see Fig. 1). The spectrum of a SCISSOR is composed of the superposition of two kinds of resonances: the ring resonance (that satisfies the condition $m_R \lambda_R = 2\pi n_{\text{eff}} R$, where m_R is the order of the resonance, λ_R is the wavelength of the resonance, n_{eff} is the effective index of the guided mode, and R is the ring radius) and the Bragg resonance due to the coherent feedback of any two rings spaced by a length satisfying a Bragg-like condition ($m_B \lambda_B = 2n_{\text{eff}} L_C$, where m_B is the resonance order and L_C is the distance between the two rings). When $L_C = m\pi R$, then $\lambda_R = \lambda_B$ and a further resonance, named CRIT, appears due to the resonant coupling of neighboring rings [6,7]. CRIT resonances are characterized by very high quality factors ($Q = \lambda/\Delta\lambda$), due to the simultaneous fulfillment of a resonance condition and an interference condition. Experimentally, CRIT resonances are observed as narrow transmission peaks in the SCISSOR stop bands [7]. The main drawback in their use is their strong dependence on fabrication imperfections, resulting in an intolerable randomness of the device spectral response [8]. The TS design allows for (a) a robust mechanism that originates the CRIT resonance

that reflects into the fabrication of a robust device against fabrication imperfections, (b) a fine control on the spectral position of the CRIT resonance, and (c) an effective switching of the CRIT resonance. The TS in Fig. 1 has rings with tapered radii: the radii of adjacent rings differ by $\pm\Delta R$. In the design discussed in this Letter, we used radii ranging from 15.050 to 14.950 μm and $\Delta R = 10$ nm. ΔR is compatible with the 3σ resolution of a deep-UV lithographic system, thus allowing the simulation of realistic devices. In the TS, the CRIT resonance is fixed by spacing two rings by a distance $L_C = \pi R$, which satisfies the constructive interference condition. All the other rings in the TS are spaced by $L_C \simeq 3/2\pi R$ [9], which yields a destructive interference. The wavelength that satisfies the constructive interference sets the CRIT resonance wavelength. Changing the pair of rings that is separated by $L_C = \pi R$ changes the CRIT resonance wavelength. Let us call the CRIT resonances the channels (CH) in our router design. Since a TS is composed of N rings, $N - 1$ pairings between adjacent rings are possible, i.e., (ideally) $N - 1$ channels can be transmitted within

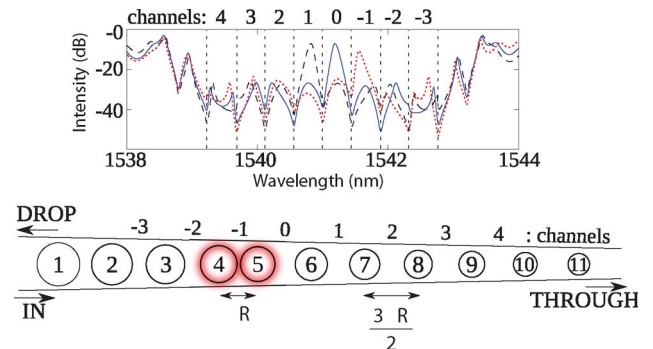


Fig. 1. (Color online) (top) Through-port signal of the TS whose structure is shown in the bottom panel. Three different TSs were simulated for different ring pairings: dashed black curve pairing of rings 6 and 7, continuous blue curve pairing of rings 5 and 6, dotted red curve pairing of rings 4 and 5. (bottom) Simplified sketch of the TS. The red circled rings show the pairing that induces the resonance for CH-1. Numbers on the top label the pairs responsible for each channel, while rings are numbered on their centers. Arrows refer to the center-to-center distance; R is defined in the text.

the TS stop band. For simplicity, in this Letter we consider that each TS routes a single channel, but with the proposed scheme at least $N/4$ channels can be routed (data not shown). In Fig. 1 pairing rings 2 and 3 identifies the channel -3, pairing rings 3 and 4 the channel -2, and so on. For the 11-ring TS, we consider only eight channels, because those ring pairings that yield resonances close to the band edges are very sensitive to disorder. Simulations of TS were performed using a standard transfer matrix code [8]. The effective modal index $n_{\text{eff}} = 1.7035 - (0.00148 \times (\lambda - 1550))$. The power coupling coefficient is a linear function of the wavelength, and it changes by about 7% over the considered wavelength range (1538–1544 nm). Ring propagation losses of 6 dB/cm are assumed, while waveguides are considered lossless. Figure 1 shows the through signal spectra for three different channels: CH-1, CH0, and CH1. It is observed that when a channel is open (i.e., the corresponding rings are paired so that CRIT occurs), the transmission in the channel is high (channel loss is -10 dB with respect to the input signal), while it is low in all the other possible channels within the TS stop band, i.e., the cross talk (through signal intensity on the adjacent channels) is lower than -20 dB. Note in Fig. 1 that the channels are densely spaced, i. e., the channel bandwidth (FWHM) is only 0.44 nm (56 GHz), which allows one to pack nine channels into 4 nm. The average ring radius determines the channel bandwidth, i.e., the channel density can be increased by increasing the ring radii, without increasing either the cross talk or the channel loss. Therefore, the TS can be used as a building block of complex router designs [10]. In order to show the TS robustness against fabrication errors, the ideal TS was perturbed by random variations of both ring radii and ring separations. A random Gaussian distribution of lengths with a zero mean and a standard deviation σ was added to the radii and the separations. Note that fabrication tolerances are usually given at $3 \times \sigma$. A statistical analysis was then performed with a metric that defines the yield of the fabrication process. In other words, we considered the probability that a CRIT resonance occurs outside its designed channel (case defined “error”) due to random length variations in the fabrication. The results of the statistical analysis are reported in Fig. 2 as an error occurrence probability (EP). Two σ values were studied: 1 and 2 nm. These σ correspond to fabrication tolerances of 3 and 6 nm, respectively. For each σ value, 500 different realizations of the same nominal TS were simulated. Figure 2 reports EP as a function of the power coupling coefficient (κ) between the waveguide and the ring. The results show that for $\kappa \geq 25\%$, EP goes to zero for $\sigma = 1$ nm and $\text{EP} < 20\%$ for $\sigma = 2$ nm. An ideal SCISSOR, with all equal R values, has a spectral response strongly dependent on κ , and $\text{EP} \gg 50\%$ is obtained (data not shown). In addition, for $\sigma = 1$ nm the range $40\% < \kappa < 45\%$ minimizes EP for all the channels while keeping the channel losses below 10 dB. Despite the strong asymmetry in the tapered structure, the channels placed symmetrically with respect to the central ring show a similar behavior: CH0 and CH1 have nearly coincident EPs, and the same applies for CH2 and CH-1. In general, CRIT channels occurring near the TS center are more insensitive to geometrical variations, while channels formed by external ring

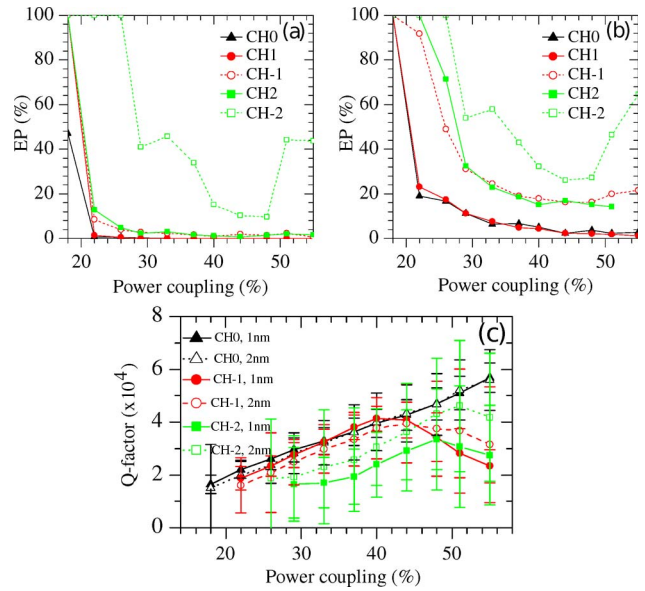


Fig. 2. (Color online) Error occurrence probability versus power coupling coefficient for various channels simulated for (a) $\sigma = 1$ nm or (b) $\sigma = 2$ nm. The labels refer to the various channels. (c) Q factor versus the power coupling coefficient for different channels and σ values. The points are the averaged values, while the bars refer to the standard deviations over 500 realizations of TS. Only values for CH0, CH-1, and CH-2 are reported, since results for CH1 = CH0, CH2 = CH-1, and CH3 = CH-2.

pairs show large EPs due to the reduced optical feedback caused by their lateral position in the TS sequence. Q factors are shown in Fig. 2(c). For the central channels, Q increases with increasing κ . For lateral channels, i. e., CH-1, CH2, and CH-2, Q initially increases and then decreases. This is due to the joint effect of a reduced optical feedback and the strong overcoupling regime that reduces the signal intensity that propagates through the TS to very low values. The net effect is to reduce the open CRIT channel intensity to values comparable to those of the other closed channels. While central channels keep their line shape, lateral channels spread in wavelength, and their Q factor decreases. With respect to the single ring resonator structure, our TS has the great advantage of maximizing its performance at high coupling coefficient values. Two important advantages arise from this fact: (1) we keep low optical losses in the device, (2) we avoid the effects related to high Q resonances and contra-directional propagating modes [11]. Another important intrinsic feature of TS is the fact that each channel can be selectively switched on/off by changing the refractive index of the rings in the pair. Unlike single resonator switches, the TS switch keeps the CRIT resonance within the channel bandwidth. Refractive index variations Δn can be achieved by electrically or optically addressing each single ring. Examples have been reported in the literature [12]. The switching of the TS channels can be achieved with either $\Delta n > 0$ or $\Delta n < 0$. However, to minimize the spectral modifications in the other channels, $\Delta n < 0$ is best for channels formed by pairing rings to the right of the central ring, while $\Delta n > 0$ is best for channels formed by pairing rings to the left of the central ring. Figure 3 reports the channel attenuation (extinction

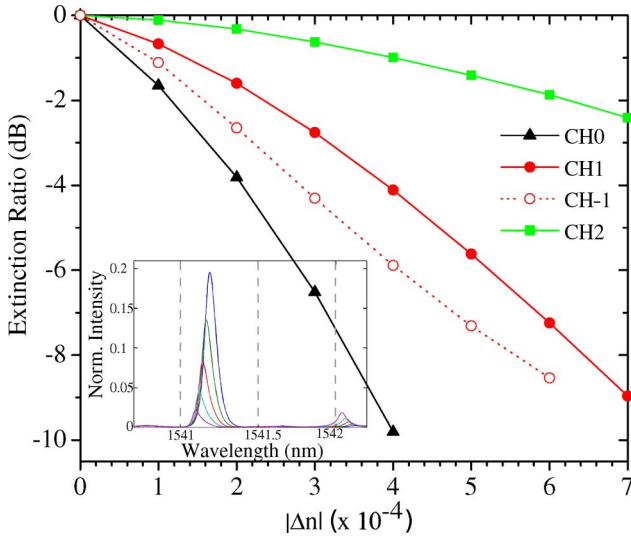


Fig. 3. (Color online) Performances of the device switching capability. Extinction ratio of the various channels versus the effective index variations of a ring pair, $|\Delta n|$. The inset shows the through spectra in the CH0 region for $|\Delta n|$ varied from 0 to 4×10^{-4} : the intensity of the CRIT peak steadily decreases with the increase of $|\Delta n|$. Dashed lines sketch the channel widths.

ratio, ER) as a function of the effective index variation $|\Delta n|$ for various channels. In this case only the four channels with the lowest EPs are considered. The inset of Fig. 3 analyzes CH0: for $|\Delta n| \rightarrow 4 \times 10^{-4}$ the CRIT resonance is attenuated by up to 10 dB, while still staying within CH0. Indeed, the strong condition for occurrence of CRIT does not allow a large resonance shift. Potentially, the switching speed is as fast as the variation of the refractive index. Thus, the ER of 10 dB for CH0 is challenging for other switching schemes (such as Mach-Zehnder interferometers or isolated ring resonators). Figure 3 reports data up to values of Δn for which the CRIT resonance is within the channel. Similar to EP, the best ER performance is achieved on the most central channels and decreases on the lateral ones: ER = -10 dB for CH0, ER < -8 dB for CH1 and CH-1, and ER ~ -2 dB for CH2. In conclusion, we described an innovative design of a tapered SCISSOR for routing and switching. The single λ channel is determined by the double condi-

tions that regulate the CRIT resonance. This stringent requirement produces a number of advantages with respect to other routing schemes: (a) a very robust design with extremely high Q factor; (b) a single channel switch mechanism that does not modify the whole TS spectrum; (c) an overcoupling working condition that relaxes the fabrication requirement on the ring to waveguide gap distance. We have discussed potential applications in optical networks, but also, applications of the proposed asymmetric SCISSOR in high-sensitivity sensors or biosensors can be envisaged due to the high Q factor.

This work was partially supported by the European Commission through the project WADIMOS (FP7-ICT-216405).

References and Notes

1. A. Shacham, K. Bergman, and L. P. Carloni, *IEEE Trans. Comput.* **57**, 1246 (2008).
2. B. G. Lee, A. Biberman, J. Chan, and K. Bergman, *IEEE J. Sel. Top. Quantum Electron.* **16**, 6 (2010).
3. S. J. B. Yoo, *Electron. Lett.* **45**, 584 (2009).
4. L. Stampoulidis, D. Apostolopoulos, D. Petrantonakis, P. Zakyntinos, P. Bakopoulos, O. Zouraraki, E. Kehayas, A. Poustie, G. Maxwell, and H. Avramopoulos, *IEEE J. Sel. Top. Quantum Electron.* **14**, 849 (2008).
5. Z. Yang and J. E. Sipe, *Opt. Lett.* **32**, 918 (2007).
6. J. E. Heebner, P. Chak, S. Pereira, J. E. Sipe, and R. W. Boyd, *J. Opt. Soc. Am. B* **21**, 1818 (2004).
7. Q. Xu, S. Sandhu, M. L. Povinelli, J. Shakya, S. Fan, and M. Lipson, *Phys. Rev. Lett.* **96**, 123901 (2006).
8. M. Mancinelli, R. Guider, M. Masi, P. Bettotti, M. R. Vanacharla, L. Pavesi, and J.-M. Fedeli, "Optical characterization of a SCISSOR device," submitted to *Opt. Express*.
9. The exact L_C value used in the simulations is $L_C = 3/2\pi R + (R_k - R) + (R_{k+1} - R)$, where R is the radius of the central ring (e.g., ring no. 6 in Fig. 1), while R_k and R_{k+1} are the radii of the two neighboring rings. This small correction to L_C is empirically used to reduce the through signal near the stop band edges.
10. M. Mancinelli, R. Guider, P. Bettotti, M. Masi, M. R. Vanacharla, and L. Pavesi, "Coupled-resonator-induced-transparency concept for wavelength routing applications," submitted to *Opt. Express*.
11. B. E. Little, J.-P. Laine, and S. T. Chu, *Opt. Lett.* **22**, 4 (1997).
12. Q. F. Xu, B. Schmidt, S. Pradhan, and M. Lipson, *Nature* **435**, 325 (2005).